Published in final edited form as:
Dev Biol. 2015 February 15; 398(2): 242–254. doi:10.1016/j.ydbio.2014.12.007.

Foxp1/2/4 regulate endochondral ossification as a suppresser complex

Haixia Zhao[1,δ], **Wenrong Zhou**[1], **Zhengju Yao**[1], **Yong Wan**[1], **Jingjing Cao**[1], **Lingling Zhang**[1], **Jianzhi Zhao**[1], **Hanjun Li**[1], **Rujiang Zhou**[1], **Baojie Li**[1], **Gang Wei**[2], **Zhenlin Zhang**[3], **Catherine A. French**[4], **Joseph D. Dekker**[5], **Yingzi Yang**[6], **Simon E. Fisher**[7], **Haley O. Iucker**[5], and **Xizhi Guo**[1,*]

[1]Bio-X Institutes, Key Laboratory for the Genetics of Developmental and Neuropsychiatric Disorders (Ministry of Education), Shanghai Jiao Tong University, Shanghai, 200240, China [δ]Development and Regeneration Key Lab of Sichuan Province, Department of Anatomy and Histology and Embryology, Chengdu Medical College, Chengdu, Sichuan Province, 610500, China [2]Shanghai Institutes for Biological Sciences, Chinese Academy of Sciences (CAS), Shanghai, 200032, China [3]Department of Orthopedic Surgery, Shanghai Jiao Tong University Affiliated the Sixth People's Hospital, Shanghai, China [4]Champalimaud Neuroscience Programme, Champalimaud Centre for the Unknown, Lisbon, Portugal [5]Institute for Cellular and Molecular Biology, University of Texas at Austin, Austin, TX 78712, USA [6]Developmental Genetics Section, National Human Genome Research Institute, NIH, 20892, USA [7]Language and Genetics Department, Max Planck Institute for Psycholinguistics, Nijmegen, The Netherlands; Donders Institute for Brain, Cognition and Behaviour, Radboud University, Nijmegen, The Netherlands

Abstract

Osteoblast induction and differentiation in developing long bones is dynamically controlled by the opposing action of transcriptional activators and repressors. In contrast to the long list of activators that have been discovered over past decades, the network of repressors is not well-defined. Here we identify the expression of Foxp1/2/4 proteins, comprised of Forkhead-box (Fox) transcription factors of the Foxp subfamily, in both perichondrial skeletal progenitors and proliferating chondrocytes during endochondral ossification. Mice carrying loss-of-function and gain-of-function *Foxp* mutations had gross defects in appendicular skeleton formation. At the cellular level, over-expression of *Foxp1/2/4* in chondroctyes abrogated osteoblast formation and chondrocyte hypertrophy. Conversely, single or compound deficiency of *Foxp1/2/4* in skeletal progenitors or chondrocytes resulted in premature osteoblast differentiation in the perichondrium, coupled with impaired proliferation, survival, and hypertrophy of chondrocytes in the growth plate. Foxp1/2/4 and Runx2 proteins interacted *in vitro* and *in vivo*, and Foxp1/2/4 repressed

*Corresponding author xzguo2005@sjtu.edu.cn; Tel/Fax: 86-021-34206736.

Runx2 transactivation function in heterologous cells. This study establishes Foxp1/2/4 proteins as coordinators of osteogenesis and chondrocyte hypertrophy in developing long bones and suggests that a novel transcriptional repressor network involving Foxp1/2/4 may regulate Runx2 during endochondral ossification.

Keywords

Foxp1; Foxp2; Foxp4; Endochondral ossification; Osteoblast; Transcriptional repressor

Introduction

The axial and appendicular skeletons form through a process of endochondral ossification. During this process, mesenchymal progenitor cells within the cartilage anlage differentiate to chondrocytes. The chondrocytes then mature through resting, proliferating, and hypertrophic stages, and are finally replaced by invading osteoblasts and blood vessels (Kronenberg, 2003). Meanwhile, skeletal progenitor cells within the perichondrium are progressively committed to an osteoblast lineage (Karsenty and Wagner, 2002; Long and Ornitz, 2013). The perichondrium is the major reservoir of osteoblast precursors in developing long bones (Maes et al., 2010), and osteoblast differentiation in the perichondrium is tightly regulated by the progressive action of osteoblast-specific transcription factors (Hartmann, 2009; Karsenty, 2008; Kobayashi and Kronenberg, 2005; Kronenberg, 2003; Long, 2012).

An array of cofactors, such as Maf, Taz, Satb2, Gli2, Dlx5, Bapx1 and Msx2, promote osteoblast differentiation by stimulating Runx2 expression or enhancing Runx2 activity (Long, 2012). Runx2 is an early transcription factor that integrates multiple osteogenic signals to induce mesenchymal progenitor cells toward osteogenic commitment (Ducy et al., 1997; Komori et al., 1997; Otto et al., 1997). During endochondral bone formation, some of these osteogenic signals come from chondrocytes. For instance, Ihh secreted by prehypertrophic and hypertrophic chondrocytes promotes osteoblast differentiation by activating Runx2. After Runx2 stimulates osteogenic commitment, Osterix and ATF4 sequentially enforce the differentiation and maturation of these osteoblasts (Ducy et al., 1996; Nakashima et al., 2002; Yang et al., 2004). Conversely, osteoblast differentiation is suppressed by repressors such as Twist1, Hand2, Zfp521, Schn3, Stat1, Tle, Hey, Hes and Hdac4, which perturb DNA binding or nuclear translocation by Runx2, decrease Runx2 protein expression, or degrade Runx2 protein (Javed et al., 2010; Long, 2012). Loss of Runx2 activators or cofactors impairs bone formation or homeostasis (Komori et al., 1997), and genetic inactivation of Runx2 repressors leads to enhanced osteoblast differentiation or ectopic ossification. For instance, *Hand2* null mice displayed enhanced ossification in the branchial arch (Funato et al., 2009).

The Fox family of transcription factors, characterized by a highly conserved forkhead DNA-binding domains, are essential for regulating several developmental processes (Augello et al., 2011; Eijkelenboom and Burgering, 2013; Katoh et al., 2013; Kume, 2011; Raychaudhuri and Park, 2011). For example, the Foxp1/2/3/4 subfamily regulates

differentiation or proliferation of cardiomyocytes (Wang et al., 2004; Zhang et al., 2010), B and T cells (Duhen et al., 2012; Feng et al., 2009; Hu et al., 2006; Wang et al., 2014), ES cells (Gabut et al., 2011) and various malignant cell-types (Chen et al., 2011; Koon et al., 2007; Korac et al., 2009). This subfamily regulates cell differentiation through transcriptional repressor activity. Foxp 1/2/4 proteins generally show overlapping expression patterns in the lung, gut, and brain during development (Lu et al., 2002; Shu et al., 2007; Takahashi et al., 2008), and in some cases, these proteins are known to act cooperatively (Li et al., 2012; Li et al., 2004). However, the role of *Foxp1/2/4* genes in bone development remains unclear. In this report, we employ genetic, histological and molecular approaches to investigate the role of *Foxp* genes during endochondral ossification. Our findings identify the Foxp1/2/4 complex as a novel Runx2 suppressor that regulates endochondral ossification.

Materials and methods

Mice

The *Foxp1*$^{fl/fl}$ (Feng et al., 2009), *Foxp2*$^{fl/fl}$ (French et al., 2007), transgenic mice *Prx1-Cre* (Logan et al., 2002) and *Col2-Cre* mice (Lu et al., 2013) have been described in previous studies. For transgenic mice generation, *Foxp1* (NM_053202.2) cDNA, *Foxp2* (BC058960) cDNA and *Foxp4* (BC057110) cDNA were individually driven by *Col2a1* promoter and enhancer as previously reported (Yang et al., 2003). The genotyping primers for the *Col2-Foxp1, Col2-Foxp2, Col2-Foxp4* and *Foxp4*$^{fl/fl}$ mice are provided in supplementary material Table S1. The genetic backgrounds of all knockout mice were uniform mixtures of 129S1/SvIMJ and C57Bl/6J. All transgenic mice were ICR background. All animal procedures were performed in accordance with protocols set by Shanghai Jiao Tong University (SYXK 2011-0112).

Generation of Foxp4 conditional knockout mice

Two *Loxp* sites were inserted into the *Foxp4* gene at introns 9 and 14 (supplemental material Fig. S4A). The targeted ES clones were identified by PCR using primers P1/P2 and P3/P4 that generate 5473 bp and 4648 bp products, respectively (supplementary material Fig. S4B). The conditional allele of *Foxp4*^{fl} is genotyped by primers P5/P6 as a 290 bp fragment. *Foxp4* was efficiently deleted by Cre activity, as evidenced by the decreased levels of *Foxp4* mRNA and protein in the E13.5 limbs from *Prx1-Cre; Foxp4*$^{fl/fl}$ *mice* (supplementary material Fig. S4D and E). Mice of homozygous *Foxp4*$^{fl/fl}$ showed no obvious abnormality throughout life, suggesting the *Foxp4*^{fl} allele functions normally.

Skeletal preparation, histological, IHC analyses and lacZ staining

Paraffin and frozen sections of skeletal samples from the transgenic and knockout mice at E15.5, E16.5 and E18.5 were obtained and processed as previously reported (Guo et al., 2004). Sections were stained as previously described using H&E for general histology (Beyotime), von Kossa for analysis of mineralization, and safranin O for analysis of proteoglycans (Guo et al., 2004). The primary antibodies for IHC were the following: anti-Osterix (1:50, Abcam, ab22552), anit-Runx2 (1:50, Santa Cruze, sc-10758), anit-Collagen Type 1:50) Ⅰ, Millipore, AB765P), anti-Foxp1 (1:50, Millipore, ABE68), anti-Foxp2 (1:200,

Abcam, ab16046), anti-Foxp4 (1:50, Milipore, ABE74), anti-Patched (1:50, Santa Cruze, sc-6149), anti-Ihh (1:50, Santa Cruze, sc-1196), anti-Flag (1:100, Agilent Technologies, 200472), anti-His (1:100, GenScript, A00174), and anti-BrdU (1:100, Abcam, ab6326). The secondary antibodies used were the Alexa Fluor 488 conjugated (1:200, Invitrogen, A-21206) and the Alexa Fluor 594 conjugated second antibody (1:200, Invitrogen, A-11058 or A-11032). Mounting was performed with DAPI fluorescent dye (Southern Biotech). Fluorescent microscopic images were taken using a Leica SP5 confocal microscope. For LacZ staining, the samples were at first performed by whole mount X-gal staining as done previously (Day et al., 2005), and then re-fixed and sectioned with 10 μm thick to observe the Cre enzyme activity.

In situ hybridization BrdU labeling and TUNEL assay

In situ hybridization for whole mount embryos or sections was performed using digoxin-labeled probes as previously described (Guo et al., 2009). Fragments of *Foxp1* (NM_053202.2) cDNA, *Foxp2* (BC058960) cDNA and *Foxp4* (BC057110) cDNA were amplified by PCR and subcloned into the pGEM-T vector to generate RNA probes, respectively. All the oligos are provided in supplementary material Table S1. Other probes have been described previously: *Sox9, Col2a1, Col10a1, Mmp13, Opn, Ihh, Pthrp, Osx, Col1a1* (Akiyama et al., 2004; Guo et al., 2004). For bromodeoxyuridine (BrdU) labeling, mice received an intraperitoneal injection of BrdU (100μg/g of body mass; Sigma). Two hours later, mice were sacrificed and embedded in paraffin for sectioning. TUNEL staining was performed using DeadEnd™ Fluorometric TUNEL System kit (Promega) according to the manufacturer's instructions.

Luciferase reporter assay, cell culture and qRT-PCR

HEK-293T or Cos7 cells with a density of 0.5×10^5 were plated in 24-well tissue and cultured until 90% confluent. Cells were transfected according to manufacturer's instructions using using lipofectamine™ 2000 (Invitrogen). Expression plasmids for p6OSE2-luc, pOG2-luc, pOG2mOSE2-luc reporter constructs have been described previously (Ducy and Karsenty, 1995). Cos7 cells were transfected with p6OSE2-luc (0.08 μg) or pOG2mOSE2-luc (0.08 μg) reporter plasmid together with the following expression plasmids as indicated: Flag-Runx2 (0.24 μg), His-Foxp1, His-Foxp2, His-Foxp4, His-Foxp1-N (0.48 μg), His-Foxp1-M (0.48 μg), His-Foxp1-N-M(0.48 μg) and His-Foxp1-C (0.48 μg). Foxp1/2/4 dose-dependent transcriptional repression of Runx2 was assayed using Foxp: Runx2 ratios of 1:3, 1:1, 2:1. HEK-293T cells were transfected with p6OSE2-luc (0.16 μg) reporter plasmid together with the following expression plasmids as indicated: Flag-Runx2 (0.16μg), Flag-Runx2-Runt (0.16 μg), His-Foxp1 (0.16 μg), His-Foxp2 (0.16 μg) and His-Foxp4 (0.16 μg). 4 ng pCMV -Renilla-luciferase plasmid (Promega) was used for normalization. Empty pcDNA3.0 vector DNA was used to equalize the total amount of DNA for all transfection assays. Luciferase assays were performed 48 hours after transfection by using the Dual Luciferase Kit (Promega).

The full-length cDNA of *Foxp4* (BC057110) or *EGFP* (used as control) were amplified by PCR and subcloned into the PMSCVpuro retroviral vector. Retrovirus was generated by transfection of PMSCVpuro-Foxp4 construct or PMSCVpuro-GFP construct into Platinum-

E Retroviral packaging cells using FuGENE 6 (Roche). ATDC5 cells were cultured in a medium of DMED/F-12 supplemented with 5% FBS (Invitrogen). To induce chondrogenic differentiation of ATDC5 cells, the cells upon reaching confluence were induced by differentiation medium by addition of insulin (10 μg/ml, Sigma), human transferrin (10 μg/ml, Sigma), and sodium selenite (10 μg/ml, Sigma). The ATDC5 cells overexpressing *Foxp4* or *GFP* protein were obtained by retroviral infection and puromycin resistance selection. Similar overexpression was performed in MC3T3 cells. MC3T3 cells were cultured in α-MEM medium (Invitrogen) including 10% FBS. For osteogenic introduction, the cells were cultured in the medium with addition of 10 mM β-glycerolphosphate (Sigma), 50 μg/ml ascorbic acid (Sigma), and 10 nM dexamethasone (Sigma). Alcian blue staining for ATDC5 cells was performed as previously report (Atsumi et al., 1990). For Alizarin Red S staining, MC3T3 Cells were fixed in 10% formalin for 30 mins and stained by 40 mM Alizarin Red S solution (pH 4.2) (Sigma).

RNA was extracted from cultured cells using the Trizol reagent (Invitrogen) according to standard procedures. SuperScript™ III First-Strand Synthesis System (Invitrogen) was used to reverse-transcribe RNA. Real-time PCR was performed on ABI Prism 7500 Sequence Detection System (Applied Biosystems) using a FastStart universial SYBR Green Master (ROX) kit (Roche). The samples were normalized to actin expression. All primer sequences for *Foxp4* quantification could be found in supplementary material Table S1.

Plasmids

The epitope-tagged derivatives of full-length *Foxp1* (NM_053202.2), *Foxp2* (BC058960), *Foxp4* (BC057110) or *Runx2* (NM_001146038), containing carboxy-terminal His, carboxy-terminal Myc or amino-terminal Flag tags as indicated , were cloned in the pcDNA3.0 vector (Invitrogen). The constructs encoding different donmains of Runx2 (NT, Runt, RunxI, NT-Runt or Runt-RunxI) or Foxp1 (N, M(LZ/ZF), C(FH), N-M(LZ/ZF)) as schematically drawn in Fig.8 or Fig.7 were amplified by PCR, and products with amino-terminal Flag tags or carboxy-terminal His tags respectively were inserted into the pcDNA3.0 vector.

Co-IP/IP assay

Co-IP assays were performed by transfecting HEK-293T cells with the indicated plasmids using lipofectamine™ 2000 (Invitrogen). After 48 hours, cells were harvested. Cell extracts were subjected to immunoprecipitation with either the anti-Myc antibody (1/2000, Roche, 11667149001), anti-His (1/2000, GenScript, A00174) or anti-Flag (1/2000, Agilent Technologies, 200472) antibody as indicated for overnight at 4°C. The antibody was coupled to protein A/G PLUS-Agrose (Santa Cruze, sc-2003). The immunoprecipitates were washed eight times with washing buffer and analyzed by SDS-PAGE and immunoblotting with antibody as indicated. For *in vivo* analysis, Nuclear extracts from E13.5 limb were immunoprecipitated with anti-Foxp1 antibody (Millipore, ABE68), anti-Foxp2 antibody (Abcam, ab16046) or IgG (Santa Cruze, sc-2027), and then blotted with anti-Foxp1 (1/1000, Millipore, ABE68), anti-Foxp2 (1/2000, Abcam, ab16046), anti-Foxp4 antibody (1/1000, Milipore, ABE74) and anti-Runx2 antibody (1/1000, Santa Cruze, sc-10758) as indicated.

Statistical analyses

Statistical analysis was performed by Student's t test using GraphPad Prism 5 software. Data are represented as means ± SEM, and significance was set at $p \leq 0.05$. For BrdU labeling, at least three individual samples analyzed and five to ten consecutive sections from each sample were taken into account.

Results

Foxp1/2/4 genes are expressed in developing long bones

Expression patterns of the *Foxp 1/2/4* genes were examined in the limb skeletons during endochondral ossification by *in situ* hybridization and immunohistochemistry (IHC). At the E12.5 stage of early skeletal primordial formation, *in situ* hybridization showed redundant expression of *Foxp1/2/4* in the digit ray of forelimbs as well as hindlimbs, partially overlapping with expression of *Sox9* and *Gdf5* in the perichondrium and joint (Figs. 1A and S1 A). Similarly, *in situ* hybridization showed redundant expression of *Foxp1/2/4* in the perichondrium/periosteum of E13.5 digits and E16.5 humerus (Figs. 1A, B). In IHC analysis of consecutive sections of E16.5 distal humerus, the range of Foxp1/2/4 expression in the perichondrium was similar to Runx2, but differed from that of the osteoblast marker Osx (arrows in Fig. 1Ca-e), implying that Foxp1/2/4 may be active in the same cell types as Runx2. Indeed, the Foxp1/2/4 proteins were mostly located in the nuclei of perichondrial cells, partially overlapping with the Runx2 distribution (arrows in Fig. S1B). In addition to the expression of Foxp1/2/4 in perichondrium, Foxp2 and Foxp4 were detected at relatively lower levels in proliferating chondrocytes (Fig. 1Cb, c). These results demonstrate that the murine *Foxp1/2/4* genes are redundantly expressed in the perichondrium and proliferating chondrocytes of developing long bones.

Over-expression of Foxp1/2/4 in chondrocytes abrogates skeletal ossification

To investigate the roles of *Foxp1/2/4* in skeletogenesis, we generated transgenic mice that overexpress *Foxp1, Foxp2,* and *Foxp4* transgenic mice in chondrocytes under the control of *Col2a1* promoter and enhancer. We obtained two or three independent founders for each transgenes. The severity of the ossification defect varied between founders with the same transgene, possibly due to the variances in copy number or ectopic expression levels of the transgene. The founders with the most severe defects were selected for further study. The over-expression of *Foxp1/2/4* in the chondrocytes of skeletons from each transgenic mouse was validated by IHC with anti-Foxp1, anti-Foxp2 or anti-Foxp4 polyclonal antibodies (Fig. S2). The *Col2-Foxp1, Col2-Foxp2* and *Col2-Foxp4* transgenic mice all showed perinatal lethality and smaller size compared to wild-type controls (Fig. 2A). The transgenes produced remarkable defects in endochondral ossification, as indicated by decreased Alizarin red staining in skeletal preparations of forelimbs and hindlimbs of transgenic mice compared to controls (Fig. 2Ab-b",c-c"). In contrast to the development of long bones, Alizarin red staining in the skulls was impaired in a relatively less extent in the transgenic embryos (Fig. 2A d-d"). Therefore, overexpression of Foxp1/2/4 in chondrocytes inhibits endochondral ossification.

The expression of *Col2a1* was relatively decreased in the chondrocytes from *Foxp* transgenic skeletons (Fig. 2Bb-b"). In addition, marked decreases of *Col10a1* (hypertrophic chondrocyte marker, Bc-c", Bg, Bg', Bi-i'), *Opn* (osteoblast marker, Fig. 2Be-e", k-k') and *Col1a1* (osteoblast marker, Figs. 2Bf-f", l-l'), safranin O (Fig. 2Ba-a") and von Kossa (Fig. 2Bd-d") staining showed greatly reduced chondrocyte hypertrophy and osteoblast differentiation in the growth plates of transgenic embryos relative to wild-type controls. Consistent with these findings, the expression of Ihh and Ptch1 were significantly abrogated in the *Col2-Foxp2* transgenic embryos (Fig. S2D). Notably, the *Col2-Foxp1* and *Col2-Foxp4* transgenic embryo appeared to retain small mineralized domains in scapula whereas the *Col2-Foxp2* mice had no mineralization at all (Figs. 2Ab'-b").

To validate the suppressive role of *Foxp* genes in chondrocyte hypertrophy and osteoblast differentiation, ATDC5 cells that are capable of undergoing a chondrogenesis *in vitro* under induction were transfected by *Foxp4*-expressing retrovirus. Compared to GFP-expressing control retrovirus, the *Foxp4*-overexpressing cells showed remarkably reduced mRNA expression of *Col10a1*, *Runx2* by 14 days post-transfection as well as lower levels *of Ptch1* and *Gli1* expression by 21 days post-transfection (Figs. S3A–C). It displayed diminished Alcian blue staining 21 days post-transfection (Fig. S3D). These results are consistent with our *in vivo* results. In addition, over-expression of *Foxp4* in MC3T3 osteoblast precursor cells repressed osteogenic differentiation, as evaluated by Alizarin red staining at 21 days post-transfection (Fig. S3E). Collectively, these findings suggest that over-expression of *Foxp1/2/4* in chondrocytes severely impairs chondrocyte hypertrophy and osteoblast differentiation.

Foxp deficiency in perichondrium and chondrocytes perturbs skeletal development

To further assess the role of *Foxp1/2/4* in cartilage and bone development, we used *Col2-Cre* to generate mice lacking *Foxp* in the perichondrium and chondrocytes. Confirming that the *Col2-Cre* mice we used have Cre activity in the perichondrium and chondrocytes, LacZ staining was evident in the perichondrium and chondrocytes of *Col2-Cre; R26R* reporter mice (Fig. S5A). The *Foxp1/2/4* genes were targeted individually or in combination, and IHC or western blot showed near-complete elimination of *Foxp* expression in the intended tissue (Fig. S4D, E and S5B). However, growth of heterozygous mice *Col2-Cre; Foxp4*$^{fl/+}$ was significantly arrested at two weeks of age, precluding the generation of homozygous *Col2-Cre; Foxp4*$^{fl/fl}$ mutant mice. Therefore, *Col2-Cre; Foxp4*$^{fl/+}$ mice were used to assess the role of *Foxp4* in long bone development. Not surprisingly, the phenotype of single knockout mice was less severe than the phenotype of the compound knockout mice. The single knockout mice survived postnatally for a long period up to one year. In contrast, *Foxp1/2* and *Foxp1/4* compound knockout mice (*Col2-Cre; Foxp1/2*$^{fl/fl}$ and *Col2-Cre; Foxp1*$^{fl/fl}$*; Foxp4*$^{fl/+}$) died perinatally, possibly due to the severe skeletal dysgenesis described below.

To analyze skeletal deformities in *Foxp* mutant mice at E18.5 and P10, overall skeletal preparations were analyzed with Alcian blue and Alizarin red staining. At E18.5, the overall body size and the appendicular skeleton were shortened in the single and compound *Foxp* mutants compared to the wild-type controls (Figs. 3A). By P10, the severity of attenuated

skeletal growth increased as the genetic dosage of *Foxp1/2* decreased (Fig. 3C). Defective skeletal development was not limited to the appendicular skeletons, as bone malformations were also detected in the skull. In the *Col2-Cre; Foxp1/2*$^{fl/fl}$ and *Col2-Cre; Foxp1*$^{fl/fl}$*; Foxp4*$^{fl+}$ compound mutants, both the cranium and nasal defects included shortened nasal bones (double head arrows) and disruption of basisphenoid bone development (yellow arrows) of the cranial base in the compound mutants (Figs. 3Ba-f). Together, these observations suggest that *Foxp* genes cooperatively regulate skeletal development in a dose-dependent manner.

To identify the molecular changes associated with defective skeletal development in the *Foxp* mutants, we performed histological and IHC analyses in sections from E18.5 tibia of mutant and control mice (Fig. 4). In the control tibia sections, von Kossa staining showed initiation of mineralization in the perichondrium/periosteum cells neighboring hypertrophic chondrocytes (outlined in Figs. 4A, A'). In contrast, in the compound *Foxp* mutant mice, we observed precocious mineralization extending to perichondrial cells neighboring the proliferating chondrocytes (marked by arrows in Figs. 4D, D', E, E'). This effect was observed, but much more subtle in the single mutant.

In agreement with these results,, osteoblast differentiation in the perichondrium was advanced in the compound mutant mice compared to the control, as indicated by the elevated expression of osteoblast markers Osx (Figs. 4I, J, 5Ag-h), ColI (Figs. 4N, O, 5Ak-l) and *Opn* (Fig. 4S, T). These findings demonstrate advanced osteoblast differentiation, maturation and mineralization during endochondral ossification in *Foxp*-deficient mice. Therefore, we hypothesized that that the *Foxp* genes may regulate osteogenic commitment.

Foxp deficiency in skeletal progenitor cells leads to precocious osteogenic commitment

To explore the effect of *Foxp* deficiency on osteogenic commitment of skeletal progenitor cells, we used *Prx1-Cre* to eliminate *Foxp* in the mesenchymal progenitor cells (Logan et al., 2002). Like the *Col2-Cre* knockout mice, which lack *Foxp* in the perichondrium and chondrocytes, the *Prx1-Cre; Foxp1/2*$^{fl/fl}$ compound knockout mice had osteogenic defects. Compound knockout of *Foxp* alleles with either *Prx1-Cre* or *Col2-Cre* resulted in relatively advanced expression of Runx2 and Osx in the perichondrium of E15.5 humerus sections (arrows in Figs. 5Aa-h, a'-h'), suggesting that *Foxp* deficiency stimulates early osteogenic induction and commitment. Moreover, ColI expression was elevated in the perichondrium adjacent to proliferating chondrocytes osteoblast maturation in the compound *Foxp* mutant, indicative of advanced osteoblast maturation (arrows in Figs. 5Ai-l, i'-l'). These results suggest that *Foxp* deficiency in the mesenchymal progenitor cells leads to a premature osteogenic commitment.

Next we tested whether *Foxp* deficiency affected osteoblast proliferation in addition to osteogenic commitment. To assess osteoblast proliferation *in vivo*, E15.5 animals were treated with BrdU, and two hours later, BrdU was quantified in the proximal humerus. IHC analyses showed that a greater percentage of osteoblast defined by Osx-expressing cells, were BrdU positive in the *Prx1-Cre; Foxp1/2*$^{fl/fl}$ mutants as compared to the *Foxp1/2*$^{fl/fl}$ controls (Figs. 5Bm' , Bn' , C). In addition, the Osx-expressing cell layers were expanded in the perichondrium of compound mutant mice compared to controls (brackets in Figs. 5Bm',

Bn', C). These results suggest that *Foxp* deficiency in mesenchymal progenitor cells led to enhanced osteoblast proliferation. Collectively, these results support the hypothesis that *Foxp* genes are important for regulating osteogenic commitment, osteoblast proliferation and differentiation during endochondral ossification.

Foxp deficiency in the perichondrium and chondrocytes impairs chondrogenesis

In addition to regulating osteogenic commitment and development, the *Foxp* genes could affect skeletal development by regulating chondrogensis. To investigate this possibility, we performed histological analyses and *in situ* hybridization on E18.5 sections from the *Col2-Cre;Foxp* mutants and controls. Safranin O staining (brackets in Figs. 6A'-E') and *Col10a1* expression (brackets in Figs. 6F–J) were used to detect collagen II and hypertrophic chondrocytes, respectively, these analyses showed smaller domains of hypertrophic chondrocytes in the growth plates of E18.5 tibia from the single and compound mutant mice compared to controls. Confirming these results, the tibia of E15.5 mutants showed a shorter distance between the two *Col10a1*-expressing domains and shorter *Opn*- and *Mmp13*-expressing domains (double head arrows in Fig. S7A), indicative of decreased chondrocyte hypertrophy. In contrast, the *Col2-Cre; Foxp1/2*$^{fl/fl}$ mutant showed an increase in proliferating or prehypertrophic chondrocytes compared to the control, assessed by expression of Ihh and Pthc1 (arrows in Fig. S7B). Therefore, *Foxp* deficiency may delay chondrocyte hypertrophy and maturation during endochondral ossification.

Next, to assess whether decreased proliferation or increased apoptosis might contribute to the reduction in hypertrophic chondrocytes, we performed the BrdU assay described above and TUNEL analysis in the proximal tibia of E18.5 mutants and the *Col2-Cre* control. Compared to the control, BrdU levels were significantly reduced in proliferating zones of all *Foxp* single and compound mutants and in the resting zones of all mutants except the *Foxp1* single mutant (Figs. 6K–O, U, V). TUNEL analysis showed significantly increased chondrocyte apoptosis in all the *Foxp* mutant mice except the *Foxp1* single mutant (Figs. 6P–T, W). Together, these data indicate that depletion of *Foxp* genes affects chondrocyte proliferation, survival and hypertrophy.

Foxp1/2/4 proteins inhibit the transacriptional activity of Runx2

The defects in endochondral ossification observed in *Foxp* deficient mice were opposite to previously described in *Runx2*$^{-/-}$ mice (Komori et al., 1997; Takarada et al., 2013). Given the overlapping expression patterns of Foxp and Runx2, we suspected that Foxp1/2/4 may influence osteogenic differentiation and chondrocyte hypertrophy by regulating Runx2. To address this possibility, we first examined the impact of Foxp proteins on Runx2 transactivation via reporter assays employing luciferase constructs (pOG2-Luc or p6OSE2-Luc) driven by consensus Runx2 binding sites in their promoters (Ducy and Karsenty, 1995). COS7 cells were transfected with the p6OSE2-Luc reporter and with Runx2 and Foxp expression vectors as indicated. As expected, co-transfection of p6OSE2-Luc and the Runx2 expression vector induced luciferase activity. Co-transfection of p6OSE2-Luc with Runx2 and Foxp1, Foxp2 or Foxp4 significantly suppressed luciferase activity, with the extent of suppression dependent on the dose of Foxp1, Foxp2 or Foxp4 (Fig. 7A). Interestingly, co-expressing various combinations of Foxp1/2/4 did not further suppress

Runx2 transactivation activity beyond the suppression caused by single Foxp proteins at the same total dose (Fig. 7B). To confirm that Foxp proteins specifically suppressed Runx2-induced luciferase activity, we repeated the assay using the pOG2mOSE2-Luc reporter, in which the Runx2 binding sites are mutated. As expected, neither Runx2 nor the Foxp proteins significantly changed the luciferase activity of this construct. These results demonstrate that Foxp proteins can suppress Runx2 transactivation activity, suggesting that Foxp complexes may function as a negative regulator of Runx2 in osteoblast lineages.

Runt is the DNA binding domain of Runx2 protein and the Runt domain alone induced luciferase activity at levels comparable to full-length Runx2 protein. Interestingly, various Foxp proteins suppressed luciferase induction by the Runt domain (Fig. 7D), suggesting that these proteins may directly bind the Runt domain of Runx2. Foxp proteins contain forkhead, leucine-zipper and zinc-finger domains, which are responsible for DNA-binding and homotypic or heterotypic proteins interactions, respectively (Wang et al., 2003). To determine which domain(s) are involved in Runx2 suppression, we created construct for expressing the Foxp1 N-terminal domain, middle domain (M, containing the leucine zipper and zinc finger domain), or C-terminal domain (containing the forkhead domain) independently or the N-terminal and middle domains together. In the luciferase assay with full-length Runx2, each domain of Foxp1 suppressed Runx2 transactivation (Fig. 7E), although no single domain suppressed Runx2 activity as effectively as the full-length protein. Collectively, these findings suggest that Foxp complexes may downregulate Runx2 activity during endochondral ossification by interacting with the Runt domain.

The Foxp1/2/4 complex interacts with Runx2

To directly test whether Foxp1/2/4 proteins can interact with Runx2, we performed co-immunoprecipitation experiments on extracts from 293T cells cotransfected with Flag-tagged Runx2 and His- or Myc-tagged Foxp constructs. As shown in Figs. 8A–C, Runx2 protein was efficiently co-immunoprecipitated with each Foxp protein. Additionally, IHC with anti-Flag and anti-His antibodies showed colocalization of Flag-tagged Runx2 and His-tagged Foxp1, 2, or 4 in the nuclei of cotransfected Cos7 cells (Fig. S8). Consistent with these *in vitro* results, endogenous Foxp1 was efficiently co-immunoprecipitated with Foxp2, Foxp4 and Runx2 in nuclear extracts from E13.5 limbs (Figs. 8D, E). These analyses demonstrate that Foxp1/2/4 proteins interact with Runx2 *in vivo* and *in vitro*.

To identify the domains involved in the interaction between Foxp1/2 and Runx2, truncated forms of Runx2 were cotransfected into Cos7 cells with Flag-tagged Runx2, and interactions were assessed by co-immunoprecipitation and His-tagged Foxp1/2/4 vectors (Fig. 8G). All forms of Runx2 that included the Runt domain interacted with Foxp2, while forms of Runx2 that lacked the Runt domain did not interact with Foxp2 (Fig. S9). Next, we used co-immunoprecipitation to test whether the Foxp1 C-terminal domain, which contains the forkhead domain, was sufficient for interactions with full-length Runx2. Indeed, the Foxp1 C-terminal domain was co-immunoprecipitated with Runx2 (Fig. 8F). Taken together, these results imply that Foxp1/2/4 bind to Runx2 via interactions between the Runx2 Runt domain and the C-terminal domain of Foxp proteins.

Discussion

In this study, we investigated the role of Foxp genes during endochondral ossification by generating transgenic mice with gain-of-function and loss-of-function Foxp mutations. Overexpression of individual Foxp1/2/4 genes disrupted osteoblast differentiation and chondrocyte hypertrophy, while single or combined deficiency of Foxp1/2/4 led to precocious ossification and defective chondrogenesis in the growth plates. Thus, the Foxp1/2/4 proteins are important for proper long bone development. Substantiating this conclusion, we found that Foxp1/2/4 expression in the perichondrium and proliferating chondrocytes of appendicular skeletons overlaps with expression of Runx2, a central regulator of endochondral ossification. Moreover, Foxp1/2/4 physically interacts with Runx2 and inhibits the transactivation function of Runx2. Collectively, these results implicate a novel pathway for the regulation of endochondral ossification.

We propose that Foxp1/2/4 proteins coordinate osteogenesis and chondrogenesis during long bone development by regulating Runx2 (Fig. 8K). This is a central factor in regulating bone development, as several repressors or corepressors, including Twist1/2, Zfp521 and Hdac4, have been reported to modulate osteoblast differentiation and chondrocyte hypertrophy through their differential interaction with Runx2 protein (Bialek et al., 2004; Correa et al., 2010; Hesse et al., 2010; Shimizu et al., 2010; Vega et al., 2004). Runx2 regulates osteoblast differentiation and chondrocyte hypertrophy partially through the induction of Ihh expression (Yoshida et al., 2004), and we detected altered Ihh signaling in the *Foxp* gain-of-function and loss-of-function mutants. Thus, dysregulated Runx2-induced Ihh signaling may account for the impaired osteoblast differentiation and chondrocyte hypertrophy in *Foxp* mutant mice.

Interestingly, *Foxp* deficiency in skeletal progenitor cells was associated with changes in Runx2 expression and cellular morphology in proliferating chondrocytes. Some proliferating chondrocytes in the *Foxp* mutants appeared to retain characteristics of prehypertrophic chondrocytes, with somewhat larger size and less organized arrangement compared to controls. In addition, expression of Runx2 and Osx were slightly elevated in perichondrium adjacent to resting or proliferating chondrocytes. Given that elevated Runx2 expression in the perichondrium has been shown to inhibit chondrocyte proliferation and hypertrophy (Hinoi et al., 2006), the gross defects in bone development in the *Foxp* mutants may result from combined regulation of Runx2 activity in the perichondrium and proliferating chondrocytes. However, it is important to note that the Foxp proteins may coordinate osteogenesis and chondrogenesis via multiple pathways, including pathways that are independent of Runx2. For example, Foxo proteins have been reported to regulate osteoblast proliferation and differentiation through interactions with Runx2, CREB and ATF4 (Almeida, 2011; Kode et al., 2012).

Furthermore, although our data support shared roles for Foxp1/2/4 proteins in regulating endochondral ossification via Runx2, there are important differences in the expression patterns and contributions of individual Foxp1/2/4 proteins during bone development. These differences suggest that the individual Foxp1/2/4 proteins play overlapping yet distinct roles in regulating osteogenic targets. For example, the overlapping expression patterns of

Foxp1/2/4, *Sox9* and *Gdf5* in early digit rays indicated that *Foxp* genes are induced early in perichondrial skeletal progenitor cells. However, *Foxp4* was preferentially expressed in the distal digit at E12.5 and E13.5, while *Foxp1* expression was relatively enriched in the perichondrium of the second phalange. *Foxp2* showed moderate expression in the perichondrium of all digits. In terms of function, deletion of a single allele of *Foxp4* by *Col2-Cre* severely arrested skeletal growth and led to osteogenic defects as severe as those caused by the dual, homozygous deletion of *Foxp2* and *Foxp1*. Yet in some cases, deletion of *Foxp2* and/or *Foxp1* had a greater effect than deletion of *Foxp4*; for example, the ectopic activation of Ihh signaling in resting/proliferating chondrocytes was more remarkable in the *Col2-Cre; Foxp1/2*$^{fl/fl}$ mutant than in the *Col2-Cre; Foxp1*$^{fl/fl}$*; Foxp4* mutant (Fig. S7B). In addition, *Foxp2* deficiency caused the most severe defects in chondrocyte proliferation while *Foxp1/4* deficiency had the greatest impact on chondrocyte apoptosis. Thus, although the Foxp1/2/4 proteins have significant redundancy and may regulate common sets of target genes as a trimeric complex, it is likely that they also play differential roles in the regulation of osteoblast differentiation and chondrogenesis, perhaps through various combinations of homoor hetero-dimers.

If distinct Foxp complexes have different roles in osteoblast differentiation and chondrogenesis, it follows that the *Foxp* genes should have context- and time-dependent functions in bone development. Indeed, while osteogenic differentiation was advanced in the long bones of the E15.5 *Prx1-Cre; Foxp1/2*$^{fl/fl}$ mutant, ossification was retarded in the parietal skull bone (Fig. S6). Thus, Foxp proteins appear to context-dependent roles in endochondral and intramembranous ossification. Thus, Foxp proteins appear to play a complex series of regulatory roles in bone development, and these roles may vary with different protein complexes, developmental stages, and tissue contexts. Additional studies will be required to fully delineate these regulatory mechanisms. In conclusion, our study suggests that Foxp1/2/4 proteins regulate endochondral ossification through their interaction with Runx2 and suppression of Runx2 activity. The study of Foxp1/2/4 provides a new transcriptional repressor that differentially control osteoblast differentiation and chondrocyte hypertrophy during long bone development.

Supplementary Material

Refer to Web version on PubMed Central for supplementary material.

Acknowledgments

Funding

This work was supported by grants to Xizhi Guo (the 973 program of China 2014CB942902 and 2012CB966903; NSFC 31171396, 31271553, 81421061 and 31100624), to Dr. Simon E. Fisher (UK Wellcome Trust, 080971) and to Dr. Haley Tucker (NIH/USA, R01CA31534).

References

Akiyama H, Lyons JP, Mori-Akiyama Y, Yang X, Zhang R, Zhang Z, Deng JM, Taketo MM, Nakamura T, Behringer RR, McCrea PD, de Crombrugghe B. Interactions between Sox9 and beta-catenin control chondrocyte differentiation. Genes Dev. 2004; 18:1072–1087. [PubMed: 15132997]

Almeida M. Unraveling the role of FoxOs in bone—insights from mouse models. Bone. 2011; 49:319–327. [PubMed: 21664311]

Atsumi T, Miwa Y, Kimata K, Ikawa Y. A chondrogenic cell line derived from a differentiating culture of AT805 teratocarcinoma cells. Cell Differ Dev. 1990; 30:109–116. [PubMed: 2201423]

Augello MA, Hickey TE, Knudsen KE. FOXA1: master of steroid receptor function in cancer. EMBO J. 2011; 30:3885–94. [PubMed: 21934649]

Bialek P, Kern B, Yang X, Schrock M, Sosic D, Hong N, Wu H, Yu K, Ornitz DM, Olson EN, Justice MJ, Karsenty G. A twist code determines the onset of osteoblast differentiation. Dev Cell. 2004; 6:423–435. [PubMed: 15030764]

Chen Z, Xiao Y, Zhang J, Li J, Liu Y, Zhao Y, Ma C, Luo J, Qiu Y, Huang G, Korteweg C, Gu J. Transcription factors E2A, FOXO1 and FOXP1 regulate recombination activating gene expression in cancer cells. PLoS One. 2011; 6:e20475. [PubMed: 21655267]

Correa D, Hesse E, Seriwatanachai D, Kiviranta R, Saito H, Yamana K, Neff L, Atfi A, Coillard L, Sitara D, Maeda Y, Warming S, Jenkins NA, Copeland NG, Horne WC, Lanske B, Baron R. Zfp521 is a target gene and key effector of parathyroid hormone-related peptide signaling in growth plate chondrocytes. Dev Cell. 2010; 19:533–546. [PubMed: 20951345]

Day TF, Guo X, Garrett-Beal L, Yang Y. Wnt/β-catenin signaling in mesenchymal progenitors controls osteoblast and chondrocyte differentiation during vertebrate skeletogenesis. Developmental Cell. 2005; 8:739–750. [PubMed: 15866164]

Ducy P, Desbois C, Boyce B, Pinero G, Story B, Dunstan C, Smith E, Bonadio J, Goldstein S, Gundberg C, Bradley A, Karsenty G. Increased bone formation in osteocalcin-deficient mice. Nature. 1996; 382:448–452. [PubMed: 8684484]

Ducy P, Karsenty G. Two distinct osteoblast-specific cis-acting elements control expression of a mouse osteocalcin gene. Mol Cell Biol. 1995; 15:1858–1869. [PubMed: 7891679]

Ducy P, Zhang R, Geoffroy V, Ridall AL, Karsenty G. Osf2/Cbfa1: a transcriptional activator of osteoblast differentiation. Cell. 1997; 89:747–754. [PubMed: 9182762]

Duhen T, Duhen R, Lanzavecchia A, Sallusto F, Campbell DJ. Functionally distinct subsets of human FOXP3+ Treg cells that phenotypically mirror effector Th cells. Blood. 2012; 119:4430–4440. [PubMed: 22438251]

Eijkelenboom A, Burgering BM. FOXOs: signalling integrators for homeostasis maintenance. Nat Rev Mol Cell Biol. 2013; 14:83–97. [PubMed: 23325358]

Feng X, Ippolito GC, Tian L, Wiehagen K, Oh S, Sambandam A, Willen J, Bunte RM, Maika SD, Harriss JV, Caton AJ, Bhandoola A, Tucker PW, Hu H. Foxp1 is an essential transcriptional regulator for the generation of quiescent naive T cells during thymocyte development. Blood. 2009; 115:510–518. [PubMed: 19965654]

French CA, Groszer M, Preece C, Coupe AM, Rajewsky K, Fisher SE. Generation of mice with a conditional Foxp2 null allele. Genesis. 2007; 45:440–446. [PubMed: 17619227]

Funato N, Chapman SL, McKee MD, Funato H, Morris JA, Shelton JM, Richardson JA, Yanagisawa H. Hand2 controls osteoblast differentiation in the branchial arch by inhibiting DNA binding of Runx2. Development. 2009; 136:615–625. [PubMed: 19144722]

Gabut M, Samavarchi-Tehrani P, Wang X, Slobodeniuc V, O'Hanlon D, Sung HK, Alvarez M, Talukder S, Pan Q, Mazzoni EO, Nedelec S, Wichterle H, Woltjen K, Hughes TR, Zandstra PW, Nagy A, Wrana JL, Blencowe BJ. An alternative splicing switch regulates embryonic stem cell pluripotency and reprogramming. Cell. 2011; 147:132–146. [PubMed: 21924763]

Guo X, Day TF, Jiang X, Garrett-Beal L, Topol L, Yang Y. Wnt/beta-catenin signaling is sufficient and necessary for synovial joint formation. Genes Dev. 2004; 18:2404–2417. [PubMed: 15371327]

Guo X, Mak KK, Taketo MM, Yang Y. The Wnt/beta-catenin pathway interacts differentially with PTHrP signaling to control chondrocyte hypertrophy and final maturation. PLoS One. 2009; 4:e6067. [PubMed: 19557172]

Hartmann C. Transcriptional networks controlling skeletal development. Curr Opin Genet Dev. 2009; 19:437–443. [PubMed: 19836226]

Hesse E, Saito H, Kiviranta R, Correa D, Yamana K, Neff L, Toben D, Duda G, Atfi A, Geoffroy V, Horne WC, Baron R. Zfp521 controls bone mass by HDAC3-dependent attenuation of Runx2 activity. J Cell Biol. 2010; 191:1271–1283. [PubMed: 21173110]

Hinoi E, Bialek P, Chen YT, Rached MT, Groner Y, Behringer RR, Ornitz DM, Karsenty G. Runx2 inhibits chondrocyte proliferation and hypertrophy through its expression in the perichondrium. Genes Dev. 2006; 20:2937–2942. [PubMed: 17050674]

Hu H, Wang B, Borde M, Nardone J, Maika S, Allred L, Tucker PW, Rao A. Foxp1 is an essential transcriptional regulator of B cell development. Nat Immunol. 2006; 7:819–826. [PubMed: 16819554]

Javed A, Chen H, Ghori FY. Genetic and transcriptional control of bone formation. Oral Maxillofac Surg Clin North Am. 2010; 22:283–293. v. [PubMed: 20713262]

Karsenty G. Transcriptional control of skeletogenesis. Annu Rev Genomics Hum Genet. 2008; 9:183–196. [PubMed: 18767962]

Karsenty G, Wagner EF. Reaching a genetic and molecular understanding of skeletal development. Dev Cell. 2002; 2:389–406. [PubMed: 11970890]

Katoh M, Igarashi M, Fukuda H, Nakagama H. Cancer genetics and genomics of human FOX family genes. Cancer Lett. 2013; 328:198–206. [PubMed: 23022474]

Kobayashi T, Kronenberg H. Minireview: transcriptional regulation in development of bone. Endocrinology. 2005; 146:1012–1017. [PubMed: 15604211]

Kode A, Mosialou I, Silva BC, Rached MT, Zhou B, Wang J, Townes TM, Hen R, DePinho RA, Guo XE, Kousteni S. FOXO1 orchestrates the bone-suppressing function of gut-derived serotonin. J Clin Invest. 2012; 122:3490–3503. [PubMed: 22945629]

Komori T, Yagi H, Nomura S, Yamaguchi A, Sasaki K, Deguchi K, Shimizu Y, Bronson RT, Gao YH, Inada M, Sato M, Okamoto R, Kitamura Y, Yoshiki S, Kishimoto T. Targeted disruption of Cbfa1 results in a complete lack of bone formation owing to maturational arrest of osteoblasts. Cell. 1997; 89:755–764. [PubMed: 9182763]

Koon HB, Ippolito GC, Banham AH, Tucker PW. FOXP1: a potential therapeutic target in cancer. Expert Opin Ther Targets. 2007; 11:955–965. [PubMed: 17614763]

Korac P, Peran I, Skrtic A, Ajdukovic R, Kristo DR, Dominis M. FOXP1 expression in monoclonal gammopathy of undetermined significance and multiple myeloma. Pathol Int. 2009; 59:354–358. [PubMed: 19432679]

Kronenberg HM. Developmental regulation of the growth plate. Nature. 2003; 423:332–336. [PubMed: 12748651]

Kume T. The Role of FoxC2 Transcription Factor in Tumor Angiogenesis. J Oncol. 2011; 2012:204593. [PubMed: 22174714]

Li S, Wang Y, Zhang Y, Lu MM, DeMayo FJ, Dekker JD, Tucker PW, Morrisey EE. Foxp1/4 control epithelial cell fate during lung development and regeneration through regulation of anterior gradient 2. Development. 2012; 139:2500–2509. [PubMed: 22675208]

Li S, Weidenfeld J, Morrisey EE. Transcriptional and DNA binding activity of the Foxp1/2/4 family is modulated by heterotypic and homotypic protein interactions. Mol Cell Biol. 2004; 24:809–822. [PubMed: 14701752]

Logan M, Martin JF, Nagy A, Lobe C, Olson EN, Tabin CJ. Expression of Cre Recombinase in the developing mouse limb bud driven by a Prxl enhancer. Genesis. 2002; 33:77–80. [PubMed: 12112875]

Long F. Building strong bones: molecular regulation of the osteoblast lineage. Nat Rev Mol Cell Biol. 2012; 13:27–38. [PubMed: 22189423]

Long F, Ornitz DM. Development of the endochondral skeleton. Cold Spring Harb Perspect Biol. 2013; 5:a008334. [PubMed: 23284041]

Lu C, Wan Y, Cao J, Zhu X, Yu J, Zhou R, Yao Y, Zhang L, Zhao H, Li H, Zhao J, He L, Ma G, Yang X, Yao Z, Guo X. Wnt-mediated reciprocal regulation between cartilage and bone development during endochondral ossification. Bone. 2013; 53:566–574. [PubMed: 23274346]

Lu MM, Li S, Yang H, Morrisey EE. Foxp4: a novel member of the Foxp subfamily of winged-helix genes co-expressed with Foxp1 and Foxp2 in pulmonary and gut tissues. Mech Dev. 2002; (119 Suppl 1):S197–S202. [PubMed: 14516685]

Maes C, Kobayashi T, Selig MK, Torrekens S, Roth SI, Mackem S, Carmeliet G, Kronenberg HM. Osteoblast precursors, but not mature osteoblasts, move into developing and fractured bones along with invading blood vessels. Dev Cell. 2010; 19:329–344. [PubMed: 20708594]

Nakashima K, Zhou X, Kunkel G, Zhang Z, Deng JM, Behringer RR, de Crombrugghe B. The novel zinc finger-containing transcription factor osterix is required for osteoblast differentiation and bone formation. Cell. 2002; 108:17–29. [PubMed: 11792318]

Otto F, Thornell AP, Crompton T, Denzel A, Gilmour KC, Rosewell IR, Stamp GW, Beddington RS, Mundlos S, Olsen BR, Selby PB, Owen MJ. Cbfa1, a candidate gene for cleidocranial dysplasia syndrome, is essential for osteoblast differentiation and bone development. Cell. 1997; 89:765–771. [PubMed: 9182764]

Raychaudhuri P, Park HJ. FoxM1: a master regulator of tumor metastasis. Cancer Res. 2011; 71:4329–4333. [PubMed: 21712406]

Shimizu E, Selvamurugan N, Westendorf JJ, Olson EN, Partridge NC. HDAC4 represses matrix metalloproteinase-13 transcription in osteoblastic cells, and parathyroid hormone controls this repression. J Biol Chem. 2010; 285:9616–9626. [PubMed: 20097749]

Shimoyama A, Wada M, Ikeda F, Hata K, Matsubara T, Nifuji A, Noda M, Amano K, Yamaguchi A, Nishimura R, Yoneda T. Ihh/Gli2 signaling promotes osteoblast differentiation by regulating Runx2 expression and function. Mol Biol Cell. 2007; 18:2411–2418. [PubMed: 17442891]

Shu W, Lu MM, Zhang Y, Tucker PW, Zhou D, Morrisey EE. Foxp2 and Foxp1 cooperatively regulate lung and esophagus development. Development. 2007; 134:1991–2000. [PubMed: 17428829]

Takahashi K, Liu FC, Hirokawa K, Takahashi H. Expression of Foxp4 in the developing and adult rat forebrain. J Neurosci Res. 2008; 86:3106–3116. [PubMed: 18561326]

Takarada T, Hinoi E, Nakazato R, Ochi H, Xu C, Tsuchikane A, Takeda S, Karsenty G, Abe T, Kiyonari H, Yoneda Y. An analysis of skeletal development in osteoblast-specific and chondrocyte-specific runt-related transcription factor-2 (Runx2) knockout mice. J Bone Miner Res. 2013; 28:2064–2069. [PubMed: 23553905]

Vega RB, Matsuda K, Oh J, Barbosa AC, Yang X, Meadows E, McAnally J, Pomajzl C, Shelton JM, Richardson JA, Karsenty G, Olson EN. Histone deacetylase 4 controls chondrocyte hypertrophy during skeletogenesis. Cell. 2004; 119:555–566. [PubMed: 15537544]

Wang B, Lin D, Li C, Tucker P. Multiple domains define the expression and regulatory properties of Foxp1 forkhead transcriptional repressors. J Biol Chem. 2003; 278:24259–24268. [PubMed: 12692134]

Wang B, Weidenfeld J, Lu MM, Maika S, Kuziel WA, Morrisey EE, Tucker PW. Foxp1 regulates cardiac outflow tract, endocardial cushion morphogenesis and myocyte proliferation and maturation. Development. 2004; 131:4477–4487. [PubMed: 15342473]

Wang H, Geng J, Wen X, Bi E, Kossenkov AV, Wolf AI, Tas J, Choi YS, Takata H, Day TJ, Chang LY, Sprout SL, Becker EK, Willen J, Tian L, Wang X, Xiao C, Jiang P, Crotty S, Victora GD, Showe LC, Tucker HO, Erikson J, Hu H. The transcription factor Foxp1 is a critical negative regulator of the differentiation of follicular helper T cells. Nat Immunol. 2014; 15:667–675. [PubMed: 24859450]

Yang X, Matsuda K, Bialek P, Jacquot S, Masuoka HC, Schinke T, Li L, Brancorsini S, Sassone-Corsi P, Townes TM, Hanauer A, Karsenty G. ATF4 is a substrate of RSK2 and an essential regulator of osteoblast biology; implication for Coffin-Lowry Syndrome. Cell. 2004; 117:387–398. [PubMed: 15109498]

Yang Y, Topol L, Lee H, Wu J. Wnt5a and Wnt5b exhibit distinct activities in coordinating chondrocyte proliferation and differentiation. Development. 2003; 130:1003–1015. [PubMed: 12538525]

Yoshida CA, Yamamoto H, Fujita T, Furuichi T, Ito K, Inoue K, Yamana K, Zanma A, Takada K, Ito Y, Komori T. Runx2 and Runx3 are essential for chondrocyte maturation, and Runx2 regulates limb growth through induction of Indian hedgehog. Genes Dev. 2004; 18:952–963. [PubMed: 15107406]

Zhang Y, Li S, Yuan L, Tian Y, Weidenfeld J, Yang J, Liu F, Chokas AL, Morrisey EE. Foxp1 coordinates cardiomyocyte proliferation through both cell-autonomous and nonautonomous mechanisms. Genes Dev. 2010; 24:1746–1757. [PubMed: 20713518]

Highlights

- *Foxp1/2/4* and *Runx2* expression overlap in the perichondrium and proliferating chondrocytes.
- Over-expression of *Foxp1/2/4* genes abrogates osteoblast differentiation and chondrocyte hypertrophy.
- Deficiency of *Foxp1/2/4* genes leads to precocious ossification and defective chondrogenesis in the growth plates.
- Foxp1/2/4 interacts with the Runx2 protein and inhibits the transcriptional activity of Runx2.

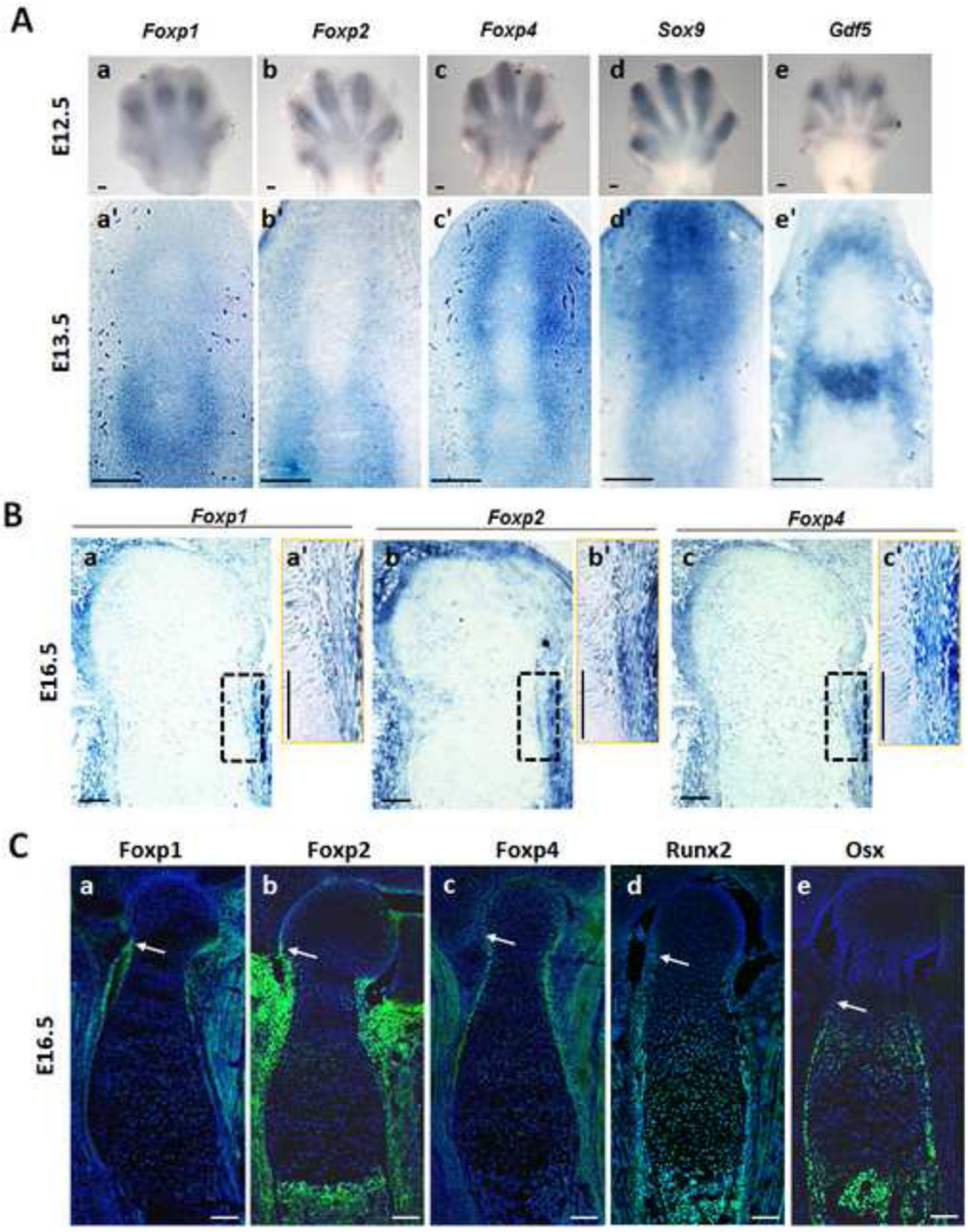

Fig. 1. Expression of *Foxp1/2/4* in the limb during skeletal development

(A) Detection *of Foxp1/2/4* expression by *in situ* hybridization in skeletal primordium at E12.5 (Aa-c) and E13.5 (Aa'-c'). Expression of *Foxp1/2/4* is mainly observed in surrounding perichondrium. Expression of *Sox9* and *Gdf5* is also shown in (Ad-e) and (Ad'-e').

(B) Detection of *Foxp1/2/4* expression in serial sections of the proximal tibia at E16.5. (Ba'), (Bb') and (Bc') show the enlargement of the boxed regions in (Ba), (Bb) and (Bc), respectively.

(C) IHC for Foxp1/2/4, Runx2 and Osterix (Osx) in serial sections of E16.5 distal humerus, counterstained with DAPI (blue). Arrows designate the onset of expression of Foxp, Runx2 and Osx, respectively, in the E16.5 proximal humerus. Scale bar: 100μm.

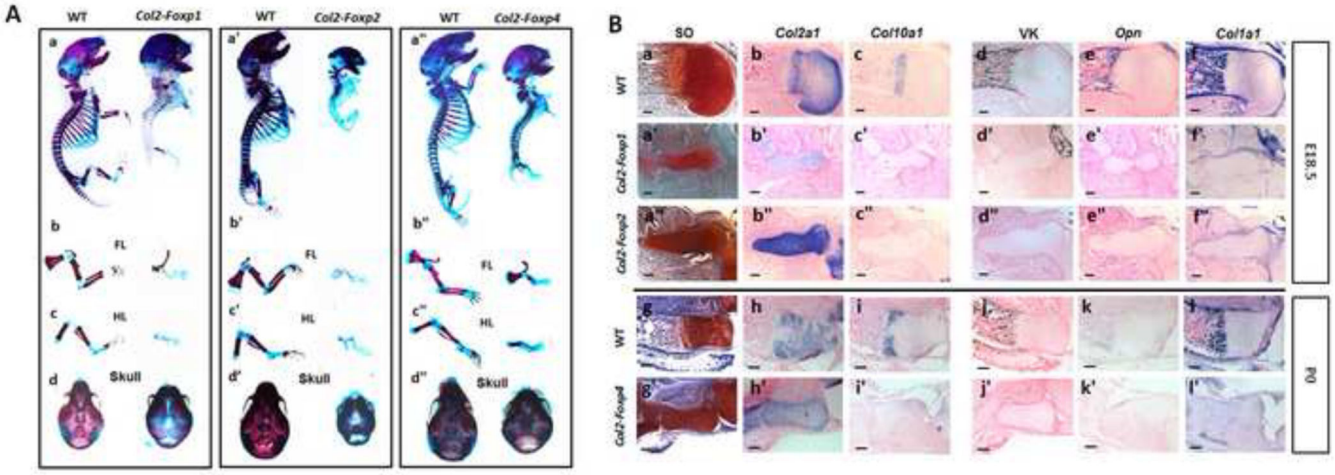

Fig. 2. Abrogated chondrocyte hypertrophy and endochondral ossification in the *Foxp1/2/4* transgenic mice

(A) Skeletal preparations from wild-type and *Col2-Foxp1/2/4* transgenic mice. Bone is stained by Alizarin red, whereas cartilage is stained by Alcian blue. Skeletons of the *Col2-Foxp1* (Aa-d) and *Col2-Foxp2* (Aa'-d') mice were examined at E18.5, whereas skeletons of the *Col2-Foxp4* (Aa"-d") mice were analyzed at P0. Lateral views of whole skeletons are shown in (Aa), (Aa') and (Aa"); forelimbs are shown in (Ab), (Ab') and (Ab"); hindlimbs are shown in (Ac), (Ac') and (Ac"); dorsal view of skulls are shown in (Ad), (Ad') and (Ad").

(B) Indicated markers of bone development were detected by *in situ* hybridization in serial sections of the E18.5 humeri from the *Col2-Foxp1/2* transgenic mice and in the P0 tibia from the *Col2-Foxp4* transgenic mice. Safranin O staining and von Kossa staining are also shown in (Ba, Ba', Ba", Bg, Bg') and (Bd, Bd', Bd",Bj, Bj'). The *Col10a1*-positive structure in Fig. 2Bc" should be the scapula. The van Kossa positive structure in 2Bd' is the clavicle. Scale bar: 200μm.

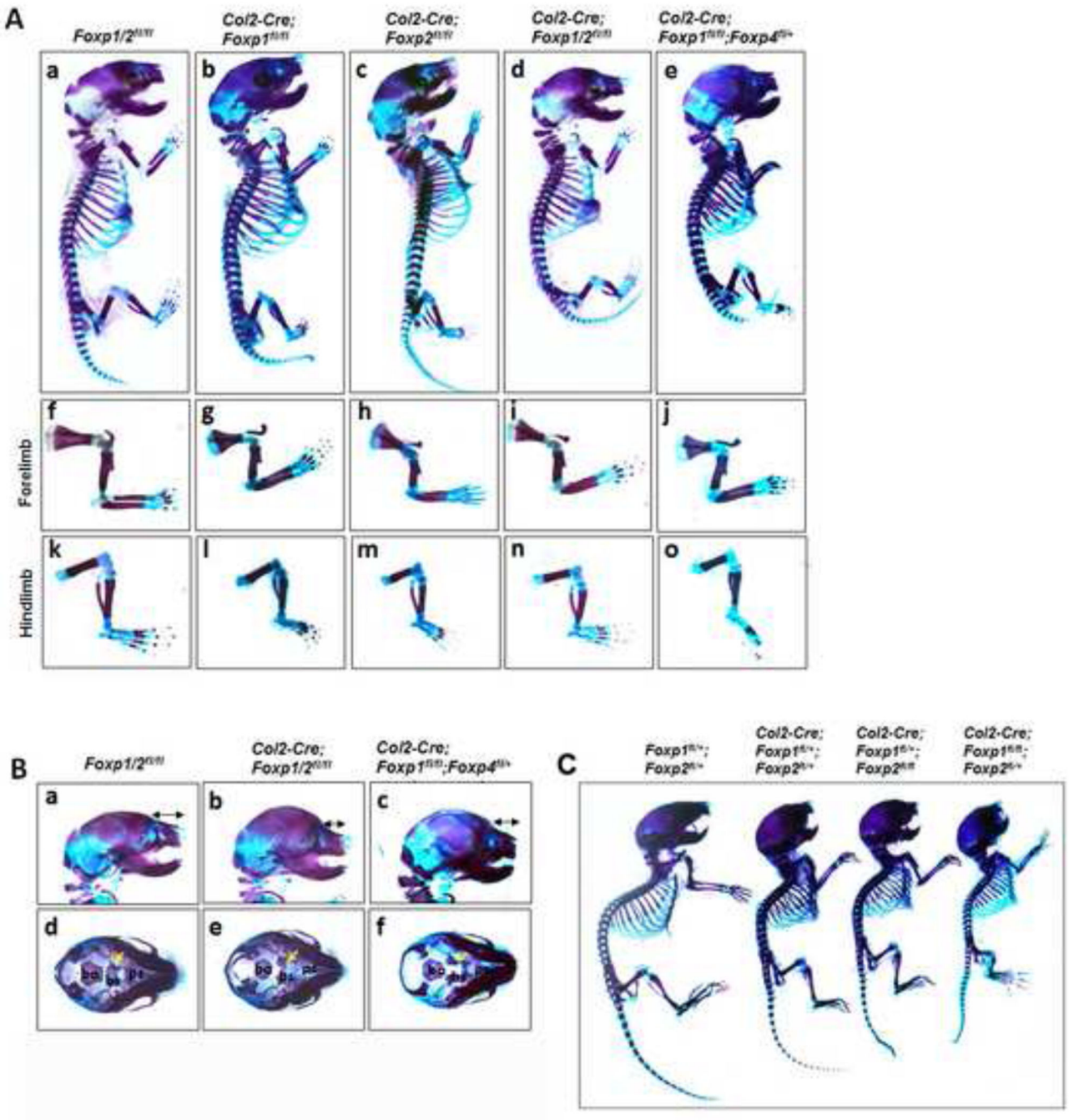

Fig. 3. Compound deficiency of *Foxp1/2/4* impairs skeletal growth

(A) Alizarin red/Alcian blue staining of skeletons isolated from the E18.5 *Col2-Cre; Foxp1*$^{fl/fl}$, *Col2-Cre; Foxp2*$^{fl/fl}$, *Col2-Cre; Foxp1/2*$^{fl/fl}$, *Col2-Cre; Foxp1*$^{fl/fl}$*; Foxp4*$^{fl/+}$ embryos, including the whole skeleton (Aa-e), forelimb (Af-j), hindlimb (Ak-o).

(B) Magnified view of E18.5 heads (Ba-f) in the *Col2-Cre; Foxp1/2*$^{f/fl}$ and *Col2-Cre; Foxp1*$^{f/fl}$*; Foxp4*$^{fl/+}$ mice, showing craniofacial malformations and shortening of the nasal bones. The formation of the cranial base bones (Bd-f, yellow arrows) is impaired in the mutants with respect to the controls. Bs, basisphenoid; bo, basioccipital; ps, presphenoid.

(C) Skeletal preparations of the P10 *Col2-Cre; Foxp1*$^{fl/+}$, *Col2-Cre; Foxp1*$^{fl/+}$*; Foxp2*$^{fl/+}$, *Col2-Cre; Foxp1*$^{fl/+}$*; Foxp2*$^{fl/fl}$, *Col2-Cre; Foxp1*$^{f/fl}$*; Foxp2*$^{fl/+}$ mice (littermates). Bone is stained with Alizarin red, whereas cartilage is stained with Alcian blue.

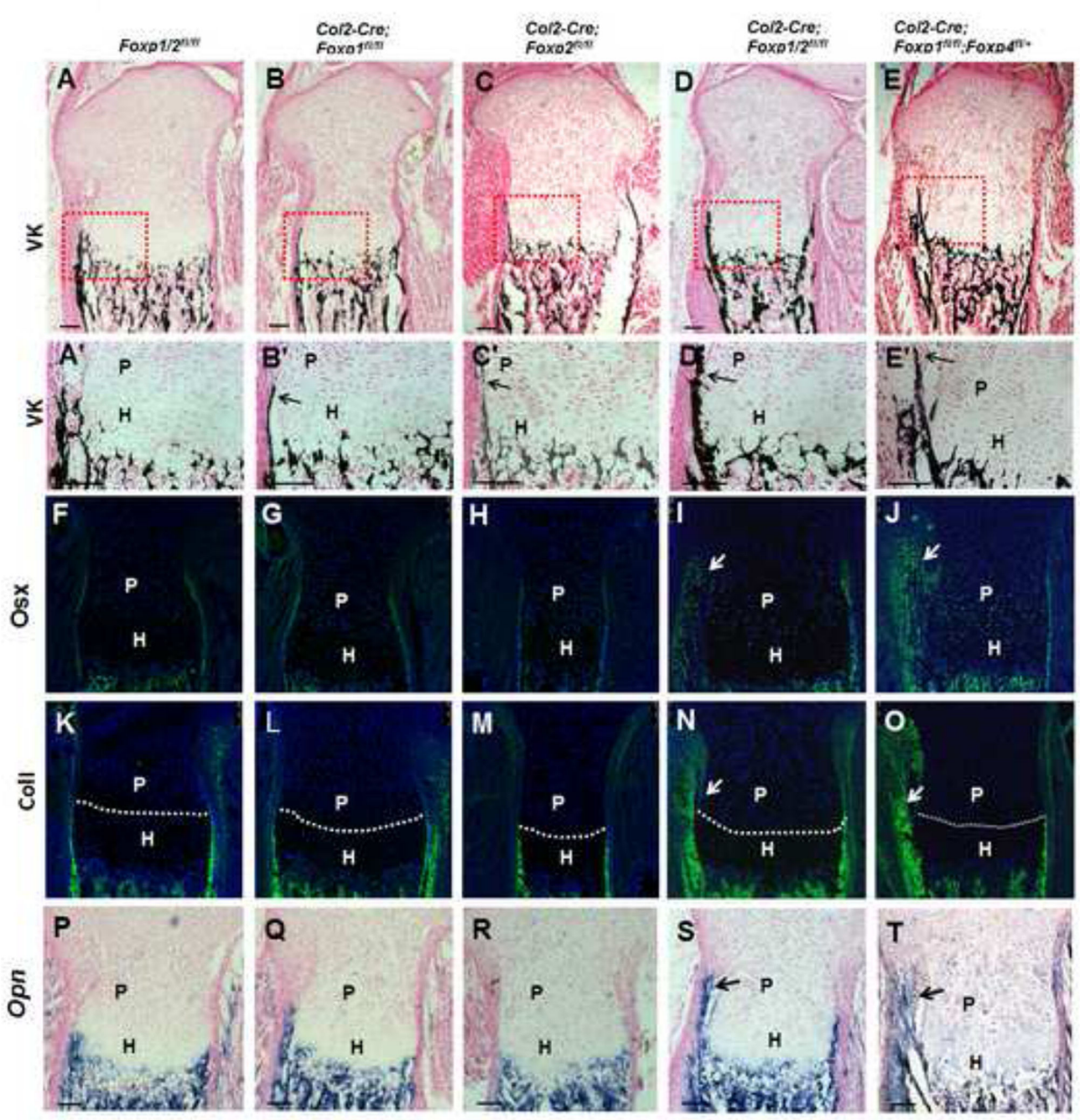

Fig. 4. Deletion of *Foxp1/2/4* by *Col2-Cre* advanced mineralization and osteoblast differentiation in the perichondrium

(A-E') Von Kossa staining of the equivalent sections of E18.5 tibiae (A–E); boxed regions are magnified in (A'-E').

(F–T) Expression of osteoblast markers Osx (F–J) and ColI (K–O) were detected by IHC, and *Opn* (P–T) was examined by *in situ* hybridization. The dashed lines delineate the proliferative/hypertrophic zone. P, proliferative zone; H, hypertrophic zone. Scale bar: 100μm.

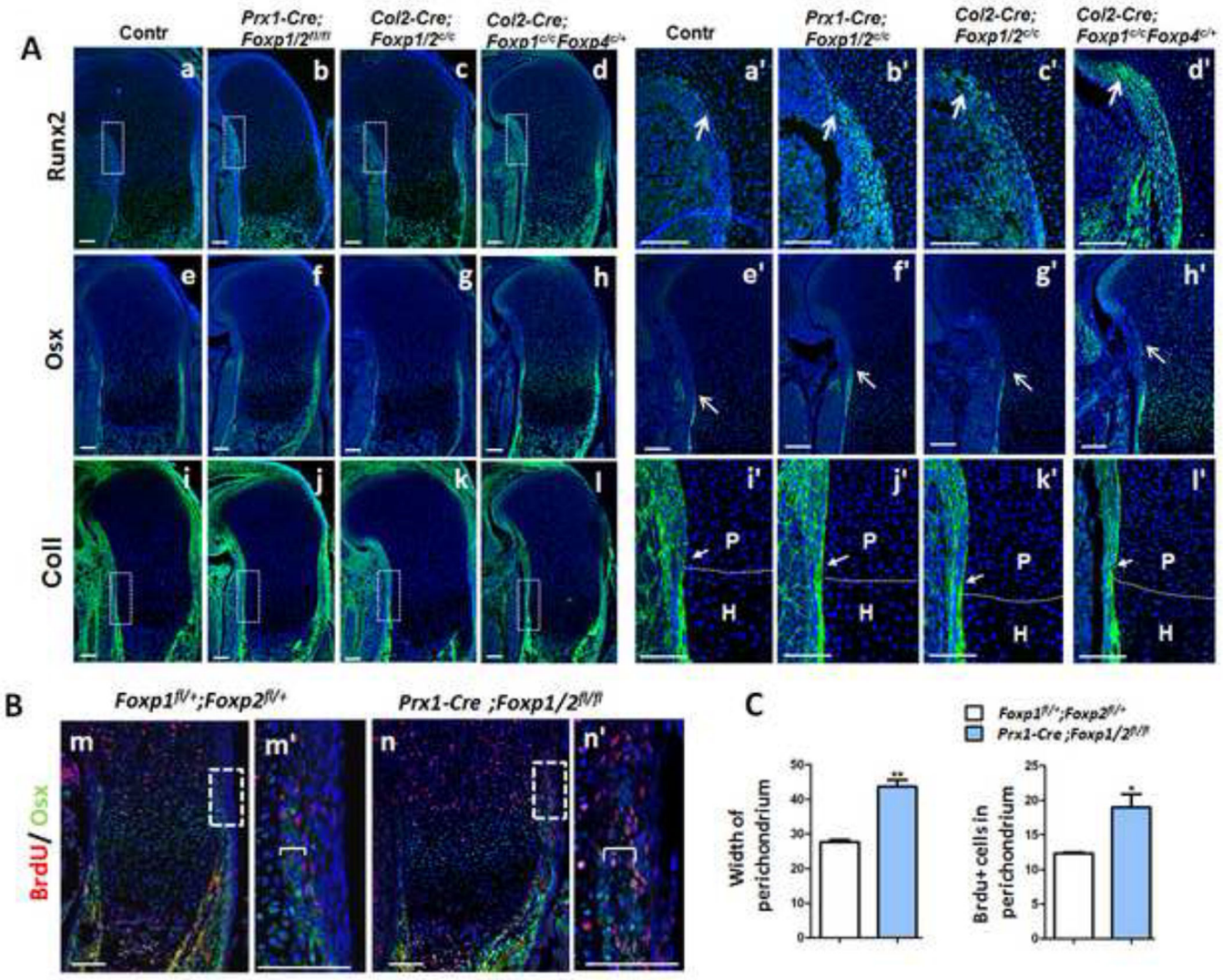

Fig. 5. Loss of *Foxp1/2/4* leads to precocious osteogenic commitment from mesenchymal progenitor cells

(A) IHC analysis of Runx2, Osx and ColI expression in equivalent sections of E15.5 humeri from the *Foxp1/2*$^{fl/fl}$ (Aa, Ae, Ai), *Prx1-Cre; Foxp1/2*$^{fl/fl}$ (Ab, Af, Aj), *Col2-Cre; Foxp1/2*$^{fl/fl}$ (Ac, Ag, Ak) and *Col2-Cre; Foxp1*$^{fl/fl}$*; Foxp4*$^{fl/+}$ (Ad, Ah, Al) embryos. The boxed regions in (Aa-d, i-l) are enlarged in (Aa'-d', i'-l'). Dashed lines delineate the proliferative/ hypertrophic zone.

(B) Double staining of BrdU (red) and Osx (green) in the equivalent sections of E15.5 humeri from *Foxp1*$^{fl/+}$*; Foxp2*$^{fl/+}$ (Bm) and *Prx1-Cre; Foxp1/2*$^{fl/fl}$ (Bn) embryos, counterstained with DAPI (blue). (Bm') and (Bn') are high-magnification images of the boxed regions in (Bm) and (Bn), respectively.

(C) Quantitative analysis indicates that the width of Osx-positive domains and the percentage of Osx-positive cells over perichondrial DAPI-positive cells are increased in the mutant (n=3). Brackets indicate the width of Osx expression regions in the perichondrium. P, proliferative zone; H, hypertrophic zone. Scale bar: 100 μm.

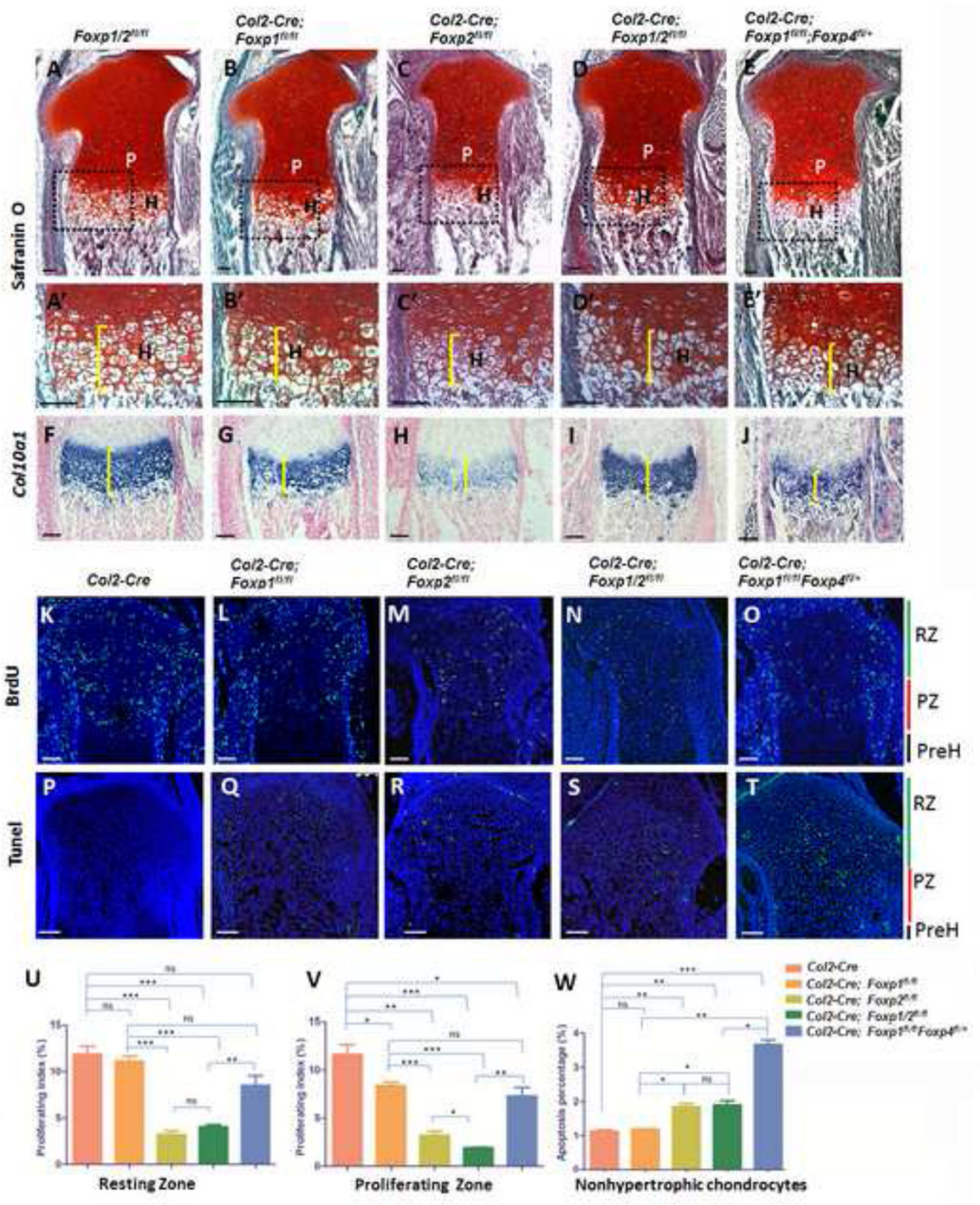

Fig. 6. Ablation of *Foxp 1/2/4* impairs chondrocyte hypertrophy

(A–E) Safrain O staining of equivalent sections in E18.5 tibiae isolated from the various *Col2-Cre; Foxp* mutant mice. P, proliferative zone; H, hypertrophic zone. (A'-E') Magnification of the boxed region in (A–E).

(F–J) Detection of *Col0a1* expression by *in situ* hybridization validates the shortened hypertrophic domains of the mutant tibiae.

(K–O) IHC for BrdU in the sections from E18.5 proximal tibiae as detected by anti-BrdU staining. RZ: the resting zone; PZ: proliferating zone; PreH: prehypertrophic zone.

(P–T) Apoptosis as detected by TUNEL assay in the sections from E18.5 proximal tibiae. RZ

(U–V) The proliferating indexes which mean the rate of BrdU-positive chondrocytes in all resting or proliferating chondrocytes in (K–O) were shown in (U) and (V), respectively.

(W) Apoptosis percentage showing the rate of TUNEL-positive cells in all nonhypertrophic chondrocytes in (P–T). n>3. ns: nonsense, (*) $p < 0.05$, (**) $p < 0.01$, (***) $p < 0.001$. Scale bar: 100μm.

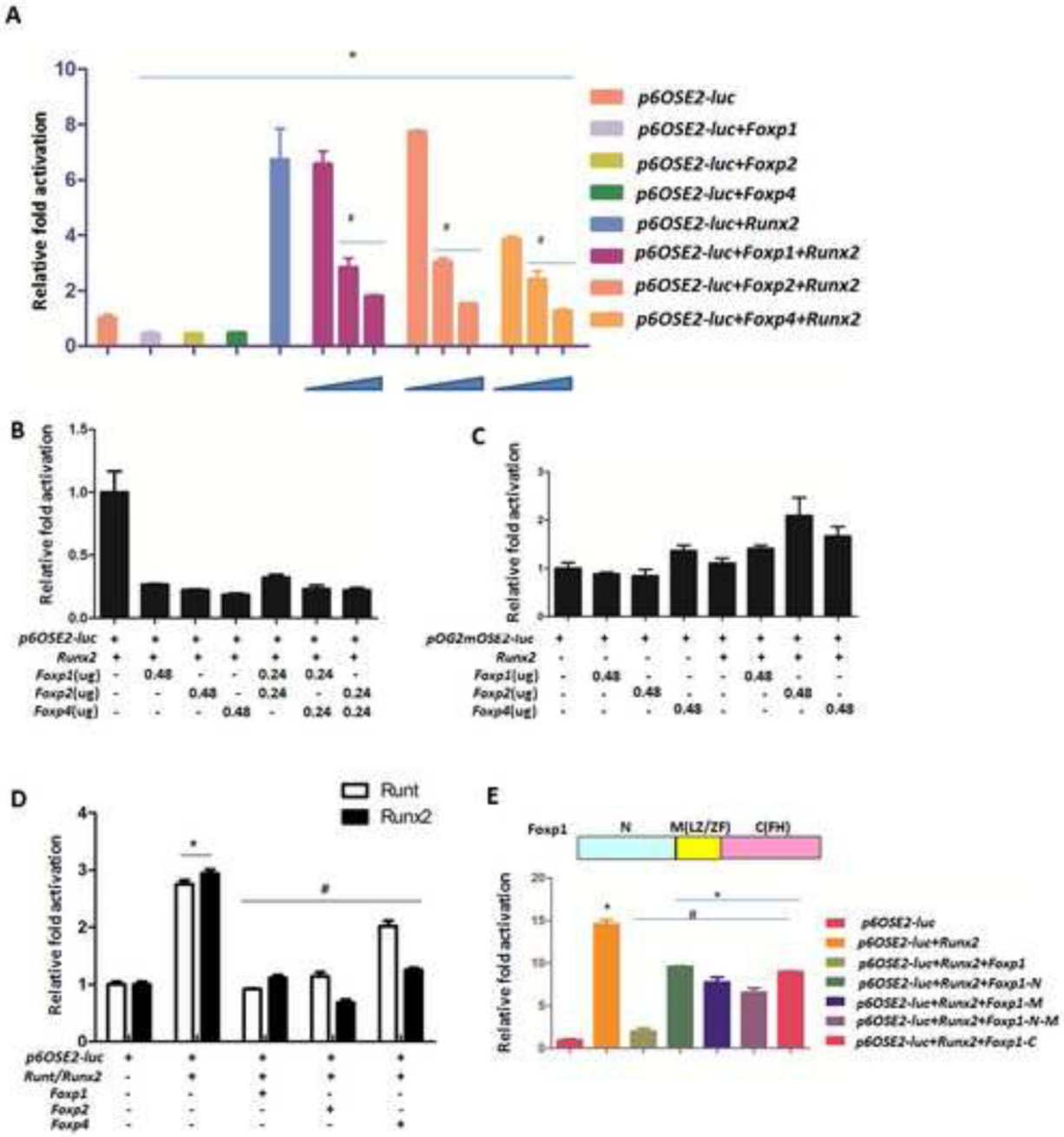

Fig. 7. Foxp1/2/4 inhibits the transcriptional activity of Runx2

(A) Transactivation by Runx2 was measured using a luciferase assay in Cos7 cells cotransfected with p6OSE2-Luc reporter (0.08 μg), Runx2 (0.24 μg) and increasing doses of Foxp1/2/4 expression constructs (at Foxp/Runx2 ratios: 1:3; 1:1; 2:1).

(B) The effects of varying combinations of Foxp1/2/4 on Runx2-induced transactivation were assessed using a luciferase assay with the pOG2-Luc reporter in Cos7 cells, as described in A.

(C) As a control, the luciferase assay was repeated in Cos7 cells using the pOG2mOSE2-Luc reporter, in which the Runx2 binding site required for Runx2 transactivation is mutated.
(D) Transient cotransfection of the p6OSE2-Luc reporter with expression vectors for Runt domain, Runx2 and Foxp1/2/4 in HEK-293T cells.
(E) Top panel: regions of Foxp1. N, N-terminus containing the poly(Q) region; M, middle, including the leucine zipper/zinc finger (LZ/ZF); and C, the C-terminal portion of Foxp1 employed for the transfections. Bottom panel: Full-length or truncated forms of Foxp1 were transiently expressed in COS7 cells co-transfected with the p6OSE2-Luc reporter and Runx2, and Runx2-induced transactivation was analyzed as above. Data are shown as mean ± SEM, and n=3. Significance was determined by *t* -test. (*) $P < 0.05$, Foxp samples versus control. (#) $P < 0.05$, Foxp samples versus Runx2 or Runt.

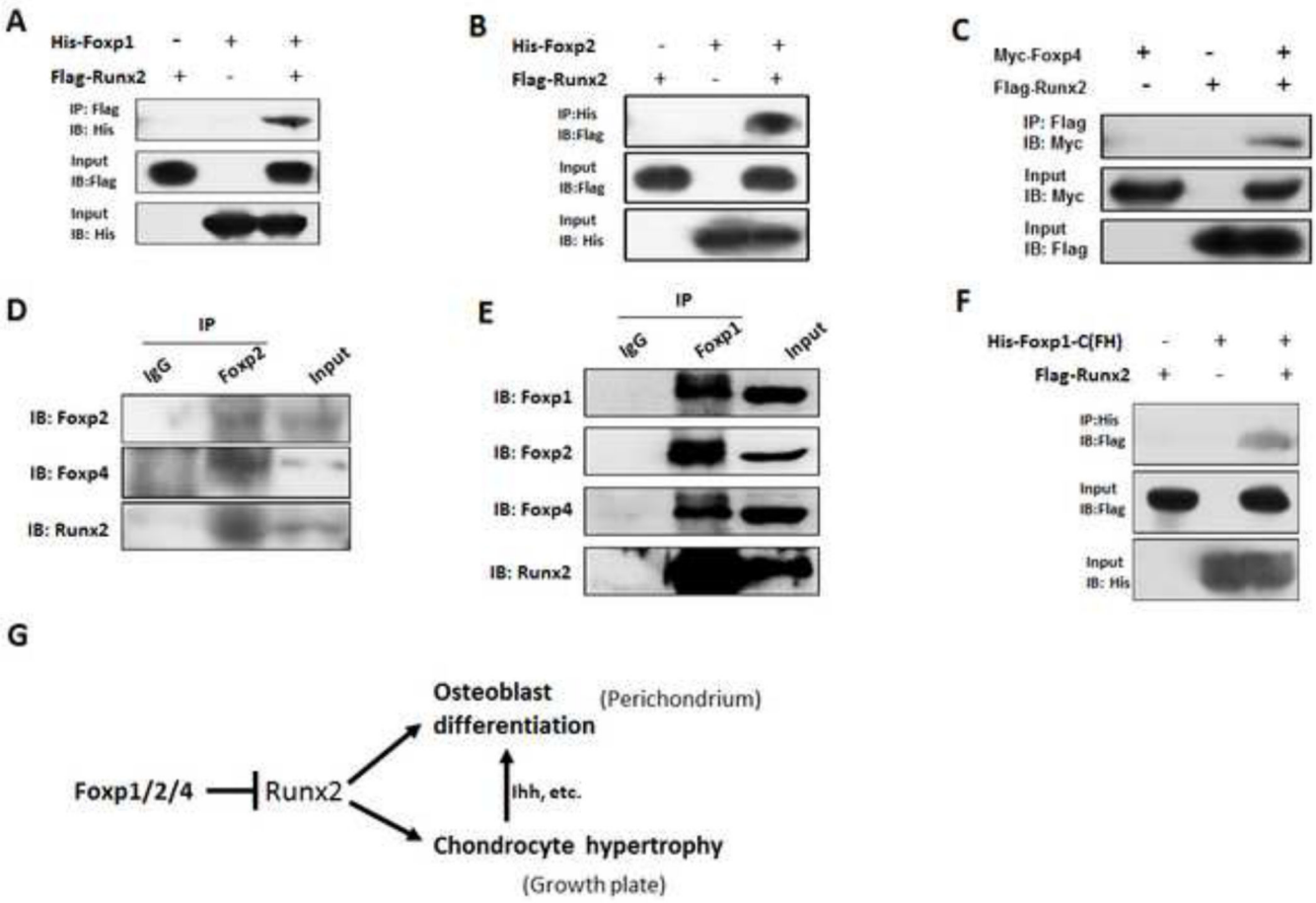

Fig. 8. Foxp1/2/4 physically interacts with Runx2

(A–C) *In vitro* interactions between Foxp1/2/4 and Runx2 were assessed by co-immunoprecipitation in HEK-293T cells cotransfected with the indicated vector combinations of His-Foxp1/Flag-Runx2 (A), His-Foxp2/Flag-Runx2 (B) or Myc-Foxp4/Flag-Runx2 (C). Cell lysates were prepared and co-immunoprecipitated with anti-Flag or anti-His and then blotted with anti-His, anti-Flag or anti-Myc.

(D-E) To assess *in vivo* interactions of endogenous Foxp and Runx2, nuclear extracts prepared from E13.5 limbs were immunoprecipitated with anti-Foxp2 or IgG and blotted with anti-Foxp2, anit-Foxp4 or anti-Runx2 antibody (D), or immunoprecipitated with anti-Foxp1 antibody and blotted with anti-Foxp1, anti-Foxp2, anti-Foxp4 or anti-Runx2 antibody (E).

(F) Runx2 co-immunoprecipitates with the C-terminal of Foxp1 containing forkhead (FH) domain (Foxp1-C). 293T cells were cotransfected with Flag-tagged Runx2 and the His-tagged Foxp1-C fragment, which included the forkhead domain (FH). Co-immunoprecipitation was performed as indicated.

(G) Proposed mechanism by which the Foxp complex regulates osteogenesis and chondrocyte hypertrophy of the growth plate: Foxp1/2/4 complex regulates osteoblast differentiation and chondrocyte hypertrophy partially through inhibiting Runx2 activity.